

Observer based Air Excess Ratio Control of a PEM fuel cell system via high order sliding mode

Alessandro Pilloni, Alessandro Pisano, *Member, IEEE*, and Elio Usai, *Member, IEEE*

Abstract—This paper deals with a high-order sliding-mode approach to the observer-based output feedback control of a PEM fuel cell system comprising a compressor, a supply manifold, the fuel-cell stack and the return manifold. The treatment is based on a lumped parameter nonlinear modeling of the PEM fuel cell system under study. The suggested scheme assumes the availability for measurements of readily accessible quantities such as the compressor angular velocity, the load current, and the supply and return manifold pressures. The control task is formulated in terms of regulating the oxygen excess ratio (which is estimated by a nonlinear, finite-time converging, high order sliding mode observer) to a suitable set-point value by using, as adjustable input variable, the compressor supply voltage. The proposed observer embeds an original synergic combination between second and third order sliding mode algorithms. The controller also uses a second order sliding mode algorithm complemented by a novel tuning procedure, supported by local linearization and frequency-domain arguments, which allows the designer to enforce a practical sliding mode regime with some pre-specified and user-defined characteristics. Thoroughly discussed simulations results certify the satisfactory performance of the proposed approach.

Index Terms—Fuel cell, observer-based output feedback, oxygen starvation, sliding mode control.

I. INTRODUCTION

Nowadays, Fuel Cells (FCs) technology is considered as a suitable option for efficient and environmentally sustainable energy conversion in many applications. However, high cost, low reliability and short lifetime of FCs are still limiting their massive utilization in real applications. Advanced control systems can be useful to achieve faster dynamic response, longer lifetime and higher efficiency of FC-based energy conversion [1], [2]. While controlling a PEM FC, one of the main problems is to estimate the oxygen excess ratio since its accurate regulation can increase the efficiency significantly [3], [4]. Unfortunately, it depends on the oxygen partial flow at the cathode $W_{O_2,in}$, which is an internal unavailable variable of the FC.

Manuscript received September 3, 2014. Accepted for publication February 12, 2015.

The research leading to these results has been partially supported by the European Community's Seventh Framework Programme FP7/2007-2013 under Grant Agreement n°257462 [Research Project "HYCON2-Network of excellence"], by the Italian Ministry for Foreign Affairs project n°PGR-00152 ["RODEO-Robust Decentralized Estimation for large-scale systems"], and by Region Sardinia project (L.R.7/2007) n°CRP-24709 ["SIAR-Sistemi Interconnessi per l'Automazione su Reti"], and n°CRP-7733 ["Sviluppo, progettazione e realizzazione prototipale di sistemi di gestione e controllo ottimali per una Micro Smart Grid"].

A. Pilloni, A. Pisano and E. Usai are with the Department of Electrical and Electronic Engineering (DIEE), University of Cagliari, Cagliari 09123, Italy.

E-mail addresses: {alessandro.pilloni, pisano, eusai}@diee.unica.it

In [5], [6], [7], [8], oxygen excess ratio regulation is indirectly achieved by controlling the air mass flow W_{cp} delivered by the compressor. Indeed, it allows to control $W_{O_2,in}$ indirectly (and, therefore, the oxygen excess ratio) once the supply manifold transient expires. The quantity W_{cp} was supposed to be available for measurement in the above works, where no state observers were used. The more recent works [5], [6], [7] exploit different high-order sliding mode (HOSM) based solutions for controlling the *breathing* FC system whereas in [8] a novel MPC-based approach to the problem is discussed.

The use of Kalman filters for the linearized model of the FC dynamics, and the adoption of integral feedback control, were suggested in [9], [10] to improve the management of the oxygen excess ratio during the transients following abrupt changes of the load current. Other types of observers such as Luenberger and adaptive ones have been also considered to estimate the state of a PEM FC [11], [12], all of them based on linearized models and therefore being quite sensitive to perturbations and modeling errors.

Sliding mode observers (SMO) do not need the process model to be linear, and are robust with respect to matched modeling errors and uncertainties as well. Furthermore, they can be implemented to estimate both the state variables and system parameters in order to achieve output feedback control and/or fault detection. An important parameter useful to know in order to avoid faulty behaviors in the FC is the water content, and in [13] it was proposed to replace the humidity sensor by a properly designed first order SMO. In [14], the proportionality constant of the inlet manifold orifice is estimated by means of a SMO and this estimated parameter is used to calculate the air mass flow-rate which is useful for control purposes.

In [15], a SMO is designed to estimate the cathode and anode pressures, while the other states (i.e., supply manifold pressure, oxygen pressure, hydrogen pressure, return manifold pressure) are estimated by a nonlinear observer. In order to implement the controller, filtering of the estimated states is needed, then finite time convergence is lost and, consequently, the lack of a separation principle must be taken into account.

Unlike other observer design approaches for nonlinear systems based on differentiation and coordinate transformation [16] or algebraic observability [17], the HOSM observer approach in [18] does not require any coordinate transformation. This approach has been extended to Multi-Output systems in [19], while some structural conditions for designing strong-observers for square and rectangular MIMO linear systems are presented in [20] and [21] respectively.

Taking advantage of the observability Brunovsky normal form, the approach in [18] has been generalized and applied

in [22] to design a discontinuous observer for a FC. In [18], that still resorts to the use of SM differentiators, a 6-th order model of the PEM FC system in which the compressor angular speed and the supply and return manifold pressures are the measured outputs, the load current is a measured disturbance, and the compressor motor voltage is the adjustable input, was considered. In the present paper, the need of sliding differentiators and peak detectors as in [22] is dispensed with, and the output injection signals of the MIMO nonlinear observer are designed by resorting to novel finite-time observer concepts [23], [24] which allow for the finite-time estimation of the FC states.

Taking into account that a kind of separation principle can be stated in the output-feedback control of nonlinear systems by using finite-time observers [25], in this paper we design the controller as an observer-based robust nonlinear controller where the considered output variable, i.e., the oxygen excess ratio, is not directly measured but evaluated using the observed internal states of the FC. The relative degree between the oxygen excess ratio and the compressor voltage is two, but since the compressor can be considered as a fast actuator with a negligible dynamics, as compared to the typical time constants of the PEM FC internal variables, a super-twisting (STW) SM controller [26] can be implemented as a nonlinear PI-like control algorithm. It is worth noting that the assumed parasitic dynamics may also include other factors such as, e.g., sensor dynamics, which enhance the importance of this approximation. The use of the STW controller for FC regulation was proposed in [27] where a pre-filter [28], [29] was used to attenuate the chattering induced by the compressor parasitic dynamics. In this paper we follow a different route and a quite simple tuning procedure (see [30]) is used to tune the STW controller gains in such a way that user's specifications on the amplitude and frequency of the steady state chattering oscillations are fulfilled.

The paper is organized as follows: in Section II the considered PEM FC non-linear model is introduced. In Section III the control objectives and the proposed control algorithm and tuning, are outlined. Section IV presents a novel HOSM-based observer for PEM FC, and its finite-time convergence properties are discussed. Section V presents the simulative validation of the proposed observer-based control architecture, including implementation issues such as model uncertainties, noisy measurements, and varying current demand. Finally Section VI provides concluding remarks and suggested directions for further related investigations.

II. OPERATIVE ASSUMPTIONS AND MODEL DESCRIPTION

A PEM FC is a complex system consisting of four main subsystems: the *hydrogen subsystem* that feeds the anode (*an*) with hydrogen (H_2), the *air-supply subsystem* (or *breathing system*) that feeds the cathode (*ca*) by air (mixture of oxygen (O_2) and nitrogen (N_2)), the *humidifier* and the *cooler* that maintain acceptable humidity degree and temperature of the FC.

For control purposes, the most complete model available in the literature has been derived by J. Pukrushpan *et al.*

TABLE I
VARIABLE OF THE NONLINEAR PEM FC MODEL

| Model variable | Symbol | Unit |
|---------------------------------|--------------------------|---------|
| Compressor motor speed | $x_1 \equiv \omega_{cp}$ | [rad/s] |
| Supply manifold pressure | $x_2 \equiv p_{sm}$ | [Pa] |
| Air mass in the supply manifold | $x_3 \equiv m_{sm}$ | [kg] |
| Oxygen mass in cathode side | $x_4 \equiv m_{O_2}$ | [kg] |
| Nitrogen mass in cathode side | $x_5 \equiv m_{N_2}$ | [kg] |
| Return manifold pressure | $x_6 \equiv p_{rm}$ | [Pa] |
| Compressor motor voltage supply | u | [V] |
| Stack current | I_{st} | [A] |

in [31]. The Pukrushpan's model is a ninth-order nonlinear model which, as commonly done, assumes the humidity degree and temperature of the inlet reactant flow to be perfectly controlled and almost constant with respect to the remaining FC variables.

In addition, since the *hydrogen subsystem* is controlled by a fast electrical valve, while the *breathing subsystem* by a slower mechanical device, a compressor (*cp*) driven by a variable speed DC motor, different time-scale decomposition might be considered [1]. Indeed, the pressure in the anode can quickly follow the changes of the cathode pressure and, therefore, the *hydrogen subsystem* dynamics can be neglected by assuming the anode pressure to be constant [4].

This assumption, along with the fair hypothesis to consider the electrical dynamic of the DC motor faster than the compressor dynamics, brings to a simplified sixth-order version of the Pukrushpan's model focused on the *breathing subsystem* [4]. Since the original Pukrushpan's model employs certain lookup tables and piece-wise continuous (but not differentiable) functions, they are replaced by appropriate smooth polynomial functions, as discussed and validated in [4], [32], [33], to meet the SM model smoothness requirements. As a result, the MIMO dynamical PEM FC model used in the present work is given by:

$$\dot{\mathbf{x}}(t) = \mathbf{f}(\mathbf{x}) + \mathbf{g} \cdot u(t) + \mathbf{s} \cdot I_{st}(t) \quad (1)$$

$$\mathbf{y}(t) = \mathbf{h}(\mathbf{x}) = [x_1(t) \quad x_2(t) \quad x_6(t)]^T \quad (2)$$

where $\mathbf{x} = [x_i] \in \mathbb{R}^6$, with $i = 1, \dots, 6$, is the vector of the state variables (defined in Table II), $u \in \mathbb{R}$ is the compressor motor control voltage, and $I_{st} \in \mathbb{R}$ is the stack current which is regarded as a measurable disturbance. The state-to-output relation is denoted as $\mathbf{h} = [h_i] \in \mathbb{R}^6 \rightarrow \mathbb{R}^3$, where as commonly assumed, only the motor speed $h_1 \equiv x_1$, and the pressures at the compressor supply and return manifolds, $h_2 \equiv x_2$ and $h_3 \equiv x_3$, are supposed to be available for measurement [4]. The vector fields $\mathbf{f} \in \mathbb{R}^6 \rightarrow \mathbb{R}^6$, $\mathbf{g} \in \mathbb{R}^6 \rightarrow \mathbb{R}$, and $\mathbf{s} \in \mathbb{R}^6 \rightarrow \mathbb{R}$ are defined as follows:

$$\mathbf{f}(\mathbf{x}) = \begin{bmatrix} f_1(x_1, x_2) \\ f_2(x_1, x_2, x_3, x_4, x_5) \\ f_3(x_1, x_2, x_4, x_5) \\ f_4(x_2, x_4, x_5, x_6) \\ f_5(x_2, x_4, x_5, x_6) \\ f_6(x_4, x_5, x_6) \end{bmatrix} \quad \mathbf{g} = \begin{bmatrix} \frac{n_{em} K_v}{J_{em} R_{em}} \\ 0 \\ 0 \\ 0 \\ 0 \\ 0 \end{bmatrix} \quad \mathbf{s} = \begin{bmatrix} 0 \\ 0 \\ 0 \\ \frac{nM_{O_2}}{4F} \\ 0 \\ 0 \end{bmatrix} \quad (3)$$

The reader is referred to the Appendix section for a complete description of the PEM FC model (1)-(3).

III. PROBLEM STATEMENT AND CONTROLLER DESIGN

A. Control Objective

The air supply management of a FC system is usually focused on maximizing the net power generated under different load conditions. This objective can be achieved by regulating the oxygen mass flow entering the stack cathode, or, equivalently, by regulating to an optimal set-point value the *oxygen excess ratio* (or *stoichiometry*)

$$\lambda_{O_2} = \frac{W_{O_2,in}(x_2, x_4, x_5)}{W_{O_2,react}(I_{st})} = \frac{W_{O_2,in}(h_2, x_4, x_5)}{W_{O_2,react}(I_{st})} \quad (4)$$

where $W_{O_2,in}$ is the oxygen partial flow in the cathode, defined in Appendix VII-B, whereas $W_{O_2,react}$, directly related to the total stack current, is the oxygen flow consumed in the reaction

$$W_{O_2,react} = M_{O_2} \frac{nI_{st}}{4F}, \quad (5)$$

in which M_{O_2} is the oxygen molar mass, n is the total number of stack's cells, and F is the Faraday constant. As discussed in [7], the optimal value $\lambda_{O_2,opt}$ can be experimentally determined from a thorough analysis of the open-loop system under various operating conditions. Experience shows that $\lambda_{O_2,opt}$ undergoes minor deviations in the different operating conditions, thus a constant set point can be considered [4].

Main advantages of constraining λ_{O_2} to an optimal value are the consistent enhancement of the FC efficiency with respect to the current demand [34] as well as the prevention of critical failures. In fact, if the starvation condition $\lambda_{O_2} < 1$ persists for a long time, the PEM FC can be irreversibly damaged.

Unfortunately, as shown in (4), the oxygen partial flow in the cathode, depends on internal variables x_4 and x_5 which are unavailable for measurements. This problem is often circumvented by inferring information from the accessible air mass flow $W_{cp}(x_1, x_2)$ delivered by compressor. Indeed once the manifold transients are expired, the relation between W_{cp} and $W_{O_2,in}$ can be identified up to a sufficient degree of accuracy (see [5] for details).

An alternative solution for reconstructing λ_{O_2} could be to measure the oxygen flow at the inlet. However, oxygen flow sensors have slow response time ($1 \div 2$ sec), short life, and low accuracy ($1 \div 10\%$) [35] which makes such an approach unsuitable. Recently, other techniques are introduced, such as measuring the inlet oxygen through volumetric relations, or by differential pressure methods, e.g. Coriolis sensors. Anyway, all these solutions are neither cheap nor able to provide satisfactory level of accuracy.

Those restrictions lead us to investigate more effective solutions to reconstruct the stoichiometry λ_{O_2} . Here, a nonlinear finite-time converging observer will be presented, which provides the condition

$$e(t) = \hat{x}(t) - x(t) = 0 \quad \forall t \geq T, T \in \mathbb{R}^+ \quad (6)$$

for some finite $T > 0$, thus achieving the exact stoichiometry reconstruction according to the formula

$$\hat{\lambda}_{O_2} = \frac{W_{O_2,in}(h_2, \hat{x}_4, \hat{x}_5)}{W_{O_2,react}(d)} \quad (7)$$

It is worth noticing that the observer converges in finite-time, then the observer/controller separation principle can be easily stated [25] and the controller using the estimated stoichiometry (7) can be designed separately from the observer. We denote the corresponding regulation error variable as

$$\hat{\sigma}(t) = \hat{\lambda}_{O_2}(t) - \lambda_{O_2,opt} \quad (8)$$

which will be steered to a vicinity of zero by a suitable SM controller whose design is outlined in the next subsection.

B. Super-Twisting Controller Design

The error variable (8) is going to be considered as the sliding variable for a second-order SM (SOSM) based control loop aimed at steering such variable to a proper vicinity of zero. In the sequel, the STW SOSM algorithm [26], whose structure is

$$\begin{aligned} u(t) &= u_1(t) + u_2(t) \\ u_1(t) &= -\rho_1 \cdot |\hat{\sigma}|^{\frac{1}{2}} \cdot \text{sign}(\hat{\sigma}) \\ \dot{u}_2(t) &= -\rho_2 \cdot \text{sign}(\hat{\sigma}), \quad \dot{u}_2(0) = 0 \end{aligned} \quad (9)$$

will be considered for controlling the FC oxygen excess ratio. The STW has become popular in the control community because, whenever applied to a sliding variable dynamics (possibly nonlinear and uncertain) having relative degree one and affine dependence on the control, it ensures disturbance rejection and finite-time convergence by means of a chattering-free continuous control action [26].

As it can be easily derived, the relative degree of the sliding variable (8) with respect to the DC motor voltage $u(t)$ is two.

Following [36], it can be noticed that the relative degree of $\hat{\sigma}$ with respect to the compressor speed x_1 is equal to one, and this can be named "principal dynamics", while the additional compressor dynamics relating x_1 and u has relative degree one and it can be considered as a "parasitic" dynamics. Although the STW algorithm guarantees the finite-time exact convergence for the rather limited class of sliding variable dynamics having relative degree one, its *practical stability* has been recently proven for a wider class of arbitrary relative degree systems admitting a certain decomposition [37], namely a relative degree one nonlinear sliding variable dynamics coupled to a sufficiently fast, possibly nonlinear, parasitic dynamics, which fits the scenario under consideration.

The STW applied to dynamics having relative degree greater than one cannot provide the attainment of an ideal sliding regime, whereas it can guarantee a permanent, self-sustained, oscillatory motion within a boundary layer of the sliding manifold. Performance analysis of the STW algorithm in presence of parasitic dynamics is currently an active research topic [28], [30], [38], [39].

A detailed frequency based analysis of the closed loop system composed of a linear, arbitrary relative degree, dynamics with the STW controller was made in [36], [39], where the describing function (DF) method was developed to analytically derive approximate values for the frequency and amplitude of the resulting self-sustained oscillation as a function of the controller parameters and plant frequency response. In [30]

a step further was made and a method for computing the STW controller parameters assigning pre-specified frequency and amplitude of the resulting self-sustained oscillation was developed. Interestingly, the method outlined in [30] only require the knowledge of the frequency response magnitude and phase at the desired frequency of self-sustained oscillation, which can be easily inspected experimentally by a simple harmonic test and, therefore, it does not require the complete knowledge of the plant transfer function.

In this work we aim to implement such a “constructive” DF based tuning procedure for (9), and to this end we rely on a linearized model between the estimated stoichiometry (7) (understood as the output) and the motor voltage (understood as input) around the desired FC operating point. We thus consider such a linearized model in the form

$$W(j\omega) = \frac{\hat{\Lambda}_{O_2}(j\omega)}{U(j\omega)} \quad (10)$$

and we aim to find a proper STW algorithm tuning such that the self-sustained steady oscillation will have a pre-specified frequency $\bar{\omega}$ and amplitude $\bar{\alpha}_y$. The procedure will successfully work if the next constraint on $\bar{\omega}$ is in force

$$\bar{\omega}_1 < \bar{\omega} < \bar{\omega}_2 \quad (11)$$

$$\arg\{W(j\bar{\omega}_1)\} = \pi/2 \quad , \quad \arg\{W(j\bar{\omega}_2)\} = \pi \quad (12)$$

The corresponding formulas for the STW parameters were derived in [30] as follows

$$\begin{bmatrix} \rho_1 \\ \rho_2 \end{bmatrix} = \begin{bmatrix} 1 \\ \Delta_1(\bar{\omega}) \end{bmatrix} \cdot \Delta_2(\bar{\omega}) \quad (13)$$

$$\begin{aligned} \Delta_1(\bar{\omega}) &= \frac{\kappa_1 \sqrt{\bar{\alpha}_y}}{\kappa_2} \cdot \tan\{\arg\{W(j\bar{\omega})\}\} \\ \Delta_2(\bar{\omega}) &= \frac{\sqrt{(\kappa_1 \bar{\alpha}_y^{1.5} \Delta_1(\bar{\omega}))^2 + (\kappa_2 \bar{\alpha}_y \Delta_1(\bar{\omega})^2)^2}}{|W(j\bar{\omega})| \cdot (\bar{\alpha}_y + \kappa_3 \Delta_1(\bar{\omega})^2)} \end{aligned} \quad (14)$$

with $\kappa_1 = 0.8986$ $\kappa_2 = 1.0282$ $\kappa_3 = 1.3091$. It is worth noting that the above formulas depend on two unknown quantities, namely the magnitude and phase of the linearized transfer function at the desired frequency of oscillation (10).

To evaluate the parameters $|W(j\bar{\omega})|$ and $\arg\{W(j\bar{\omega})\}$, a simple procedure to build an harmonic test is devised. At first, by means of iterative simulation runs, the constant control value $u = U_0$ is searched in such a way that the corresponding steady state value of the oxygen excess ratio coincides with the set point $\lambda_{O_2,opt}$ for a value of the stack current I_{st} placed in the middle of the admissible range. Since in practice the oxygen excess ratio is not measurable, the estimate given by the finite time converging observer that will be designed in the next section will be considered. After that, the control is changed to $u = U_0 + U_1 \sin(\bar{\omega}t)$, and the resulting harmonic oscillation of the (estimated) oxygen excess ratio is analyzed to extract the corresponding magnitude and phase of the associated (linearized) transfer function corresponding to the selected working condition of the system. The above procedure is designed in such a way that it could be also implemented in practice. In spite the suggested procedure is approximate, in the sense that it relies on a local linearization of the nonlinear relationship between the DC motor voltage $u(t)$ and the oxygen excess ratio $\lambda_{O_2}(t)$, the simulation results

presented in the sequel will show that such an approximation is largely satisfied and, in fact, we will be able to impose desired frequency and amplitude of the steady state oxygen excess ratio oscillation up to an unexpected degree of accuracy.

Transient specifications on the error variable can be imposed too. The response time can be generally reduced by increasing the value of the tuning parameters. This reduction process has an intrinsic limit that actuator saturation may take place when the chosen parameters are too large. Overshoot cannot be avoided using the Super-Twisting, whose trajectories in the error phase plane “rotate” around the origin by construction. Overshoot reduction, however, can be achieved, if needed, by shaping the set-point signal according to the known “reference governor” paradigm widely used in linear and nonlinear control. Another possibility to affect at the same time transient and steady-state response specifications can be that of using a certain set of tuning parameters during transient, and then smoothly change them, at the end of the transient, to those values providing satisfactory steady state performance. This “gain adaptation” procedure, however, require dedicated analysis as it could induce unwanted instability phenomena.

IV. PEM FC OBSERVER DESIGN

In this section a HOSM observer able to reconstruct in finite-time the whole state of the PEM FC and useful for both control and fault prevention will be described. It is worth to stress that the proposed observer does not require the implementation of any differentiator to guarantee the annihilation of the estimation error. Apart from the output injection design, the theoretic framework supporting the observer design is the same as in [22] and it is briefly resumed for the reader convenience.

The observer is designed as a replica of the system model (1)-(3), without any coordinate transformation, plus a properly defined output injection function:

$$\dot{\hat{\mathbf{x}}}(t) = \mathbf{f}(\hat{\mathbf{x}}) + \mathbf{g} \cdot u(t) + \mathbf{s} \cdot I_{st}(t) + \mathcal{O}_{sq}(\hat{\mathbf{x}})^{-1} \cdot \zeta(\mathbf{e}_y) \quad (15)$$

$$\hat{\mathbf{y}}(t) = \mathbf{h}(\hat{\mathbf{x}}) = [\hat{x}_1(t) \quad \hat{x}_2(t) \quad \hat{x}_6(t)]^T \quad (16)$$

where $\hat{\mathbf{x}} \in \mathbb{R}^n$ is the estimated state ($n = 6$), $\mathbf{e}_y = \mathbf{h}(\hat{\mathbf{x}}) - \mathbf{h}(\mathbf{x}) \in \mathbb{R}^p$ is the output error ($p = 3$), and $\zeta(\mathbf{e}_y) \in \mathbb{R}^n$ is the output injection vector. $\mathcal{O}_{sq}(\cdot) \in \mathbb{R}^{n \times n}$ is a nonsingular square mapping, chosen by selecting n linearly independent rows from the system’s observability matrix $\mathcal{O}(\mathbf{x})$.

To compute $\mathcal{O}_{sq}(\mathbf{x})$, n independent rows have to be chosen from the $p(n-p+1)$ rows of the system observability matrix, which for the PEM FC model (1)-(3) takes the form

$$\mathcal{O}(\mathbf{x}) = \begin{bmatrix} d\mathbf{h}(\mathbf{x}) \\ dL_{f(\mathbf{x})}^1 \mathbf{h}(\mathbf{x}) \\ dL_{f(\mathbf{x})}^2 \mathbf{h}(\mathbf{x}) \\ dL_{f(\mathbf{x})}^3 \mathbf{h}(\mathbf{x}) \end{bmatrix} \in \mathbb{R}^{12 \times 6} \quad (17)$$

where $d = \partial/\partial \mathbf{x} = [\partial/\partial x_1, \dots, \partial/\partial x_n]$ is the gradient operator, $L_{f(\mathbf{x})} \mathbf{h}(\mathbf{x}) = (\partial \mathbf{h}(\mathbf{x})/\partial \mathbf{x}) \cdot \mathbf{f}(\mathbf{x})$ is the Lie derivative of $\mathbf{h}(\mathbf{x})$ along $\mathbf{f}(\mathbf{x})$, and the k -th derivative of $\mathbf{h}(\mathbf{x})$ along $\mathbf{f}(\mathbf{x})$ is defined recursively as $L_{f(\mathbf{x})}^k \mathbf{h}(\mathbf{x}) = (\partial L_{f(\mathbf{x})}^{k-1} \mathbf{h}(\mathbf{x})/\partial \mathbf{x}) \cdot$

$\mathbf{f}(\mathbf{x})$. Among the all possible selections $\mathcal{O}_{sq,\ell}(\mathbf{x})$ ($\ell = 1, 2, \dots$) that can be obtained starting from (17), i.e.

$$\mathcal{O}_{sq,\ell}(\mathbf{x}) = \begin{bmatrix} \frac{\partial h_1(\mathbf{x})^T}{\partial \mathbf{x}} & \dots & \frac{\partial L_{\mathbf{f}}^{r_1,\ell-1} h_1(\mathbf{x})^T}{\partial \mathbf{x}} & \frac{\partial h_2(\mathbf{x})^T}{\partial \mathbf{x}} & \dots \\ \dots & \frac{\partial L_{\mathbf{f}}^{r_2,\ell-1} h_2(\mathbf{x})^T}{\partial \mathbf{x}} & \frac{\partial h_2(\mathbf{x})^T}{\partial \mathbf{x}} & \dots & \frac{\partial L_{\mathbf{f}}^{r_3,\ell-1} h_3(\mathbf{x})^T}{\partial \mathbf{x}} \end{bmatrix}^T$$

where the integers $r_{k,\ell}$ must satisfy the relation $\sum_{k=1}^3 r_{k,\ell} = 6$, we are going to choose the one that is not singular in the largest subset of the state-space containing the nominal working conditions of the PEM FC.

Due to the high complexity of the observability matrices $\mathcal{O}_{sq,\ell}(\mathbf{x})$, which are state-dependent and strongly nonlinear, the full rank condition will be numerically checked by solving the following off-line multidimensional optimization problem

$$\max_{\ell} \min_{\mathbf{x} \in \mathbf{X}} \det(\mathcal{O}_{sq,\ell}(\mathbf{x}))^2 \quad (18)$$

where $\det(\mathcal{O}_{sq,\ell}(\mathbf{x}))^2$ is the squared determinant of each candidate matrix. Since the problem (18) is not convex, the optimization algorithm used for solving (18) was based on the well known MATLAB “fminsearch” algorithm. To avoid numerical singularities, the final selection has been done in accordance with the requirements that the minimum of the cost function associated with the matrix must be sufficiently far from zero.

Thanks to the aforementioned optimal criterion, the set of optimal indices were found as $r_{1,\ell^*} = 1$, $r_{2,\ell^*} = 2$ and $r_{3,\ell^*} = 3$, which gives rise to the following nonsingular mapping

$$\mathcal{O}_{sq,\ell^*}(\mathbf{x}) = \begin{bmatrix} \frac{dh_1(\mathbf{x})}{d\mathbf{f}h_2(\mathbf{x})} \\ \frac{dh_2(\mathbf{x})}{d\mathbf{f}h_3(\mathbf{x})} \\ \frac{dL_{\mathbf{f}}h_2(\mathbf{x})}{dL_{\mathbf{f}}h_3(\mathbf{x})} \end{bmatrix} = \begin{bmatrix} 1 & 0 & 0 & 0 & 0 & 0 \\ 0 & 1 & 0 & 0 & 0 & 0 \\ \mathbf{d}f_2(x_1, x_2, x_3, x_4, x_5) \\ 0 & 0 & 0 & 0 & 0 & 1 \\ \mathbf{d}f_6(x_4, x_5, x_6) \\ \mathbf{d}L_{\mathbf{f}}f_6(x_4, x_5, x_6) \end{bmatrix} \quad (19)$$

Let then $\mathcal{O}_{sq}(\mathbf{x}) = \mathcal{O}_{sq,\ell^*}(\mathbf{x})$ and $r_k = r_{k,\ell^*}$ with $k = 1, 2, 3$. It remains to properly design the injection vector defined as

$$\zeta(\mathbf{e}_y) = [\zeta_{1,1} \quad \zeta_{2,1} \quad \zeta_{2,2} \quad \zeta_{3,1} \quad \zeta_{3,2} \quad \zeta_{3,3}]^T \in \mathbb{R}^6 \quad (20)$$

By subtracting (1)-(3) from (15)-(16), (19), the observation error dynamics is

$$\dot{\mathbf{e}}(t) = \mathbf{f}(\hat{\mathbf{x}}) - \mathbf{f}(\mathbf{x}) + \mathcal{O}_{sq}(\hat{\mathbf{x}})^{-1} \zeta(\mathbf{e}_y) \quad (21)$$

$$\mathbf{e}_y(t) = \mathbf{h}(\hat{\mathbf{x}}) - \mathbf{h}(\mathbf{x}) \quad (22)$$

Thus, deriving the expression for the successive derivatives of each output error e_{y_k} up to the order r_k , it yields:

$$e_{y_k}^{(j)} = L_{\mathbf{f}(\hat{\mathbf{x}})}^j h_k(\hat{\mathbf{x}}) - L_{\mathbf{f}(\mathbf{x})}^j h_k(\mathbf{x}) + \zeta_{k,j}(v_k), \quad 1 \leq j \leq r_k \quad (23)$$

Considering that $\mathbf{x} = \hat{\mathbf{x}} - \mathbf{e}$, in accordance with Lemma 1 in [18], (22) and (23) allow for constructing the following diffeomorphism

$$\boldsymbol{\epsilon} = \Phi(\mathbf{e}, \hat{\mathbf{x}}) = \begin{bmatrix} \Phi_1(\mathbf{e}, \hat{\mathbf{x}}) \\ \Phi_2(\mathbf{e}, \hat{\mathbf{x}}) \\ \Phi_3(\mathbf{e}, \hat{\mathbf{x}}) \end{bmatrix} \quad (24)$$

preserving the origin, i.e. such that $\Phi^{-1}(\mathbf{0}, \hat{\mathbf{x}}) = \mathbf{0} \quad \forall \hat{\mathbf{x}} \in \mathbf{X}$, and where the sub-blocks $\Phi_k = [\varphi_{k,j}] \in \mathbb{R}^{r_k}$, with $\varphi_{k,1} \equiv e_{y_k}$,

$k = 1, 2, 3$ and $j = 1, \dots, r_k$, have the following canonical component-wise representation

$$\begin{cases} \tilde{\varphi}_{k,1} &= \varphi_{k,2} + \zeta_{k,1} \\ \vdots &= \vdots \\ \tilde{\varphi}_{k,r_k-1} &= \varphi_{k,r_k-1} + \zeta_{k,r_k-1} \\ \tilde{\varphi}_{k,r_k} &= \tilde{\varphi}_{k,r_k+1} + \zeta_{k,r_k} \end{cases} \quad (25)$$

with $\tilde{\varphi}_{k,r_k+1} = L_{\mathbf{f}(\hat{\mathbf{x}})}^{r_k} h_k(\hat{\mathbf{x}}) - L_{\mathbf{f}(\mathbf{x})}^{r_k} h_k(\mathbf{x})$, $k = 1, 2, 3$. Taking into account the real FC behavior, any bounded error in the state estimation implies bounded drift terms $\tilde{\varphi}_{k,r_k+1}$, i.e.,

$$|\hat{\mathbf{x}} - \mathbf{x}| \leq \varepsilon \quad \Rightarrow \quad |\tilde{\varphi}_{k,r_k+1}(\hat{\mathbf{x}}, \mathbf{x})| \leq \Pi_i \quad (26)$$

and then each output error dynamics (25) can be independently stabilized by resorting to suitable HOSM algorithms. Since we have three sub-dynamics respectively of order one, two, and three, we design the first output injection entry as the STW algorithm (27), the injection term for the second-order block as a STW based velocity observer (28), see [25], whereas the third and last dynamics will be stabilized by employing the novel continuous third-order SM control algorithm in (29), whose stability properties have been recently analyzed in [23], [24].

$$\begin{aligned} \zeta_{1,1}(t) &= -\lambda_1 \cdot |\varphi_{1,1}(t)|^{\frac{1}{2}} \text{sign}(\varphi_{1,1}(t)) + \zeta_{1,2}(\varphi_{1,1}(t)) \\ \zeta_{2,2}(t) &= -\lambda_2 \cdot \text{sign}(\varphi_{1,1}(t)) \quad , \quad \zeta_{1,2}(0) = 0 \end{aligned} \quad (27)$$

$$\begin{aligned} \zeta_{2,1}(t) &= -\alpha_1 \cdot |\varphi_{2,1}(t)|^{\frac{1}{2}} \text{sign}(\varphi_{2,1}(t)) \\ \zeta_{2,2}(t) &= -\alpha_2 \cdot \text{sign}(\varphi_{2,1}(t)) \end{aligned} \quad (28)$$

$$\begin{aligned} \zeta_{3,1}(t) &= -\beta_1 L \cdot |\varphi_{3,1}(t)|^{\frac{2}{3}} \text{sign}(\varphi_{3,1}(t)) \\ \zeta_{3,2}(t) &= -\beta_2 L^2 \cdot |\varphi_{3,1}(t)|^{\frac{1}{3}} \text{sign}(\varphi_{3,1}(t)) \\ \zeta_{3,3}(t) &= -\beta_3 L^3 \cdot \text{sign}(\varphi_{3,1}(t)) \end{aligned} \quad (29)$$

It is worth to remark that, in contrast to all existing third order SM controllers, algorithm (29) is able to steer to zero a perturbed third-order integrator dynamic as in (25)-(26) without employing any nested differentiator, but employing only the output estimation error $\varphi_{3,1} = \hat{x}_6 - x_6$. Furthermore, dispensing with the use of differentiators considerably reduces the complexity of the algorithm [23], [24], and enhances its robustness to the measurement noise.

With reference to the stability analysis of the proposed observer, since the three subsystems (25) are decoupled, the finite-time converging of the underlying output error $\varphi_{k,1}$ and their derivatives up to order r_k can be guaranteed by independently chosen positive parameters sets, respectively (λ_1, λ_2) , (α_1, α_2) and $(\beta_1, \beta_2, \beta_3, L)$. Thus, denoted $[\varphi_{k,j}]^z = |\varphi_{k,j}|^z \cdot \text{sign}(\varphi_{k,j})$ and $z \in \mathbb{R}^+$, following [23], [24], [25], the next positive definite quadratic function

$$V(\Phi) = \sum_{k=1}^3 \zeta_k(\Phi_k)^T P_k \zeta_k(\Phi_k) \succ 0 \quad (30)$$

with $P_k \in \mathbb{R}^{r_k \times r_k}$ positive definite and $\zeta_k(\Phi_k)$ defined as

$$\zeta_1(\Phi_1) = [|\varphi_{1,1}|^{\frac{1}{2}} \quad \varphi_{1,2}]^T \quad (31)$$

$$\zeta_1(\Phi_2) = [|\varphi_{2,1}|^{\frac{1}{2}} \quad \varphi_{2,2}]^T \quad (32)$$

$$\zeta_1(\Phi_3) = [|\varphi_{3,1}|^{\frac{2}{3}} \quad \varphi_{3,2} \quad |\varphi_{3,3}|^2]^T \quad (33)$$

can be made a strict Lyapunov function for the whole error dynamics (25)-(29). The detailed tuning procedure of the injection term gains can be found in [23], [25]. It is worth to

remark that, since all of the three error dynamics converges to zero in finite-time, then the observer is able to reconstruct the whole state of the PEM FC in finite-time too. Consequently, the separation principle is automatically satisfied and the oxygen excess ratio controller and the FC observer can be separately designed.

Remark 1: Taking into account the robustness property of the SM approach with respect matched uncertainty and disturbance, the evaluation of the equivalent control by filtering the output injections variables $\zeta_{i,i}$ allows for implementing also a FDI module [18], [16] for MIMO systems.

V. SIMULATION RESULTS

A number of case studies were analyzed to verify the effectiveness of the proposed observer-based control scheme in the presence of parameter uncertainty and noisy measurements. The nominal model parameters were set on the basis of data reported in [4], [32], [33]. The corresponding values, listed in Appendices VII-D and VII-E, correspond to a 75-kW high pressure FC stack fed by a 14-kW turbo compressor used in the Ford P2000 FC electric vehicle. Simulations were performed in the MatLab/Simulink environment using Euler fixed-step solver with sampling time $T_s = 0.1\text{msec}$. In agreement with standard performances of modern μ -controller/DSP architectures [40], [41] and AD/DA interfaces [42], [43], both the data acquisition and the proposed observer-based control scheme operate at 5msec of sampling rate.

A brief description of the simulations is now presented. In TEST 1 the FC is fed in open-loop by a constant voltage, the aim of this test being that of verifying the convergence features of the observer. In TEST 2 the loop is closed by means of the proposed controller (9). No parameter uncertainty in the observer is considered for this test. For investigating the performance deterioration arising from a mismatch between the actual and the nominal parameters employed into the observer, some parameter uncertainties are included in TEST 3. Finally, TEST 4 investigates the performance under the simultaneous effect of parameter uncertainties and noisy measurements. The operating range for the load current is $0 \div 200$ [A], and the adopted current demand is $I_{st}(t) = 100\text{A}$ for $t \in [0, 15)$, 150A for $t \in [15, 25)$, 120A for $t \in [25, 35)$, 190A for $t \in [35, 45)$.

In accordance with the previously discussed stability analysis, a feasible choice for the injection terms parameter (27)-(29) is as follows (see [23], [24]): $\lambda_1 = 110$, $\lambda_2 = 5$, $\alpha_1 = 110$, $\alpha_2 = 5$, $\beta_1 = 13.2$, $\beta_2 = 50.82$, $\beta_3 = 13.31$ and $L = 2$.

Figure 1 shows a comparison between the actual and estimated profiles of the unmeasured variables x_3, x_4, x_5 during TEST 1, in which the PEM FC was fed by a constant voltage $u = 132$ [V]. The fast convergence of the observer and its high estimation accuracy are both evident. TEST 2 shows the resulting closed loop results. The optimal stoichiometry value for the considered FC is $\lambda_{O_2,opt} = 2.06$, see [4], [33]. In order to apply the “frequency-based” tuning procedure outlined in Section III-B, the stack current I_{st} is set in the middle of the admitted operating range, i.e. 100 [A], and it has been found iteratively the constant voltage $u = U_0$ guaranteeing the optimal stoichiometry value $\lambda_{O_2,opt}$, yielding $U_0 = 132$ [V]. After

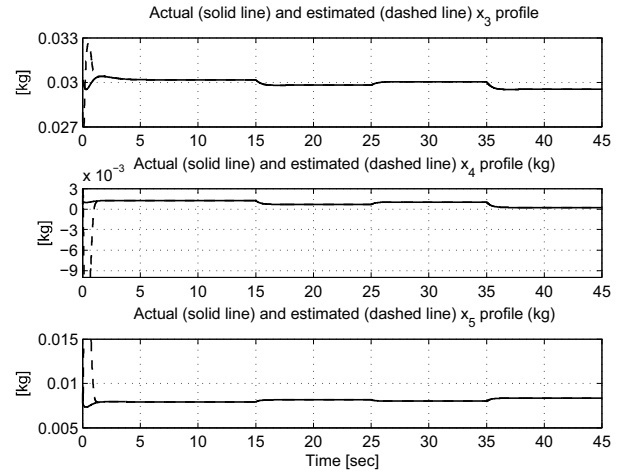


Fig. 1. Actual and observed profiles of variables x_3, x_4, x_5 in TEST 1

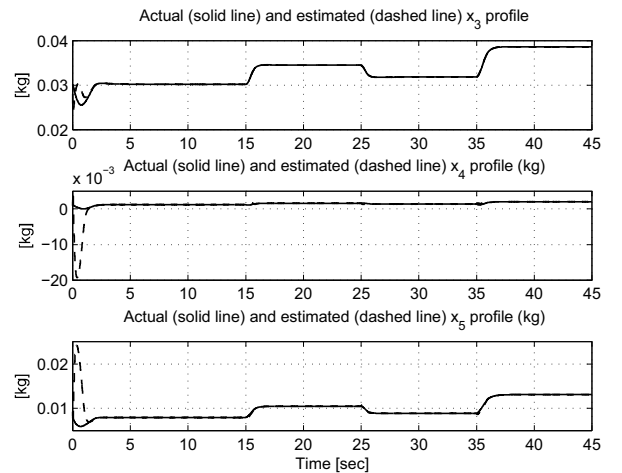


Fig. 2. Actual and observed profiles of variables x_3, x_4, x_5 in TEST 2

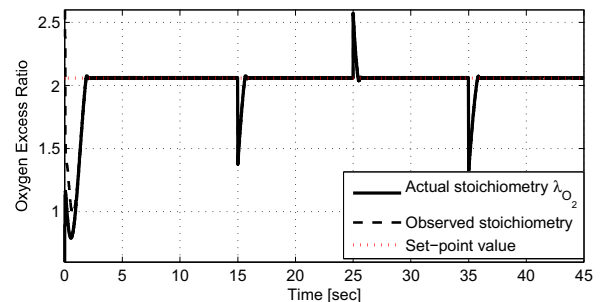


Fig. 3. Actual and observed λ_{O_2} , and set-point value, in TEST 2

that, we have arbitrarily chosen the frequency and amplitude of the self-sustained oscillation as $\bar{\omega} = 2\pi \cdot 6$ [rad/sec] and $\bar{\alpha}_y = 2 \times 10^{-3}$. Then, by a simple harmonic test, carried out by feeding the system with the voltage $u(t) = U_0 + 10 \cdot \sin(\bar{\omega}t)$, the following values of magnitude and phase for the linearized model (10) are obtained: $|W(j\bar{\omega})| = 6.704 \times 10^{-4}$ and $\arg\{W(j\bar{\omega})\} = -138.46$ [deg], respectively. Finally, by

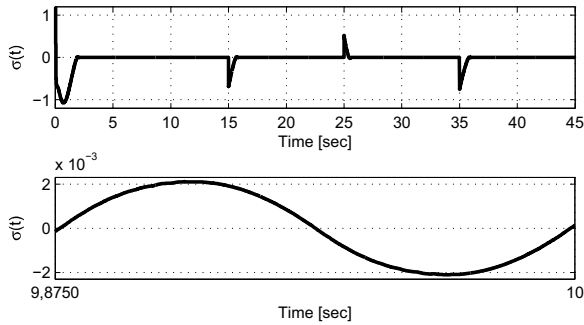


Fig. 4. Stoichiometry error steady-state behavior in TEST 2

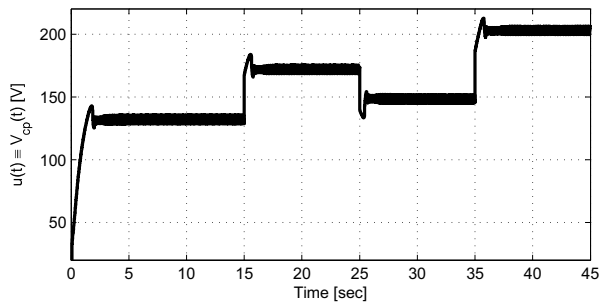


Fig. 5. Compressor supply voltage in TEST 2

applying the tuning rules (14), the gains of the STW controller (9) were evaluated as $\rho_1 = 44.8712$ and $\rho_2 = 78.0974$. It is worth to remark that this procedure is basically experiment-based and it does not require the knowledge of the plant transfer function (10), thus it can be easily implemented in practice. Figure 2 shows the actual and estimated profiles of the unmeasured variables x_3 , x_4 , x_5 . The observer correctly works in the closed loop as well.

Figure 3 focuses on the performance of the control loop by showing the actual and estimated stoichiometry along with the corresponding set-point value. Fast dynamics and high accuracy of the control loop are evident. Figure 4-top reports the profile of the sliding manifold (8), whereas Figure 4-bottom shows a zoom from which it is apparent that the steady-state accuracy and self-sustained motion due to presence of parasitic actuator dynamic match the pre-specified magnitude and frequency values. Figure 5 depicts the applied compressor motor voltage.

In TEST 3, the performance of the proposed observer/controller under parameter uncertainties is verified. Fol-

 TABLE II
 VARIATION OF SYSTEM PARAMETERS

| Parameter | Nominal Value | Variation |
|---|--------------------|-----------|
| Stack Temperature (T_{st} [K]) | 353 | +10% |
| Ambient temperature (T_{amb} [K]) | 298 | +10% |
| Supply manifold volume (V_{sm} [m ³]) | 0.02 | -10% |
| Return manifold volume (V_{rm} [m ³]) | 0.005 | -10% |
| Compressor diameter (d_c [m]) | 0.2286 | +1% |
| Compressor/motor inertia (J_{cp} [kg/m ²]) | 5×10^{-5} | +10% |

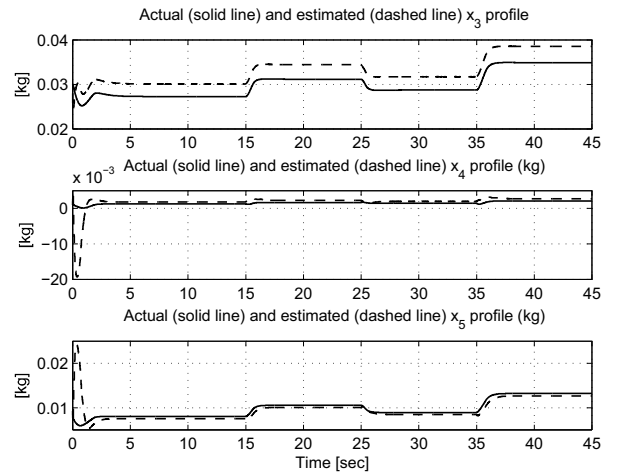
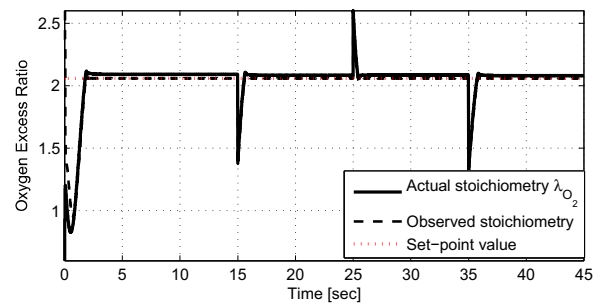
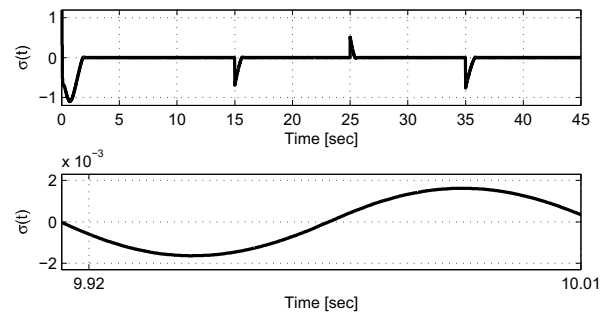
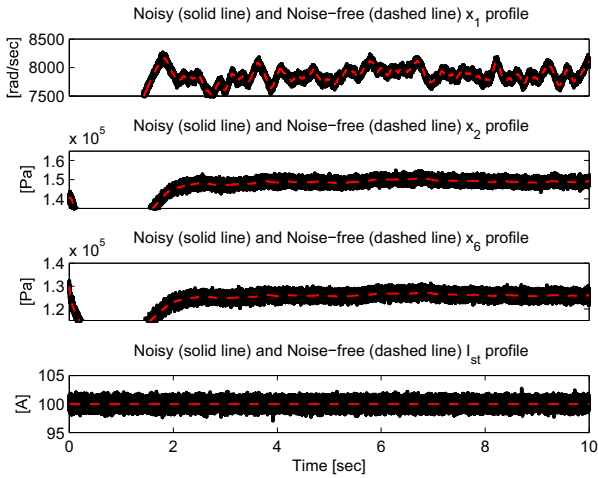
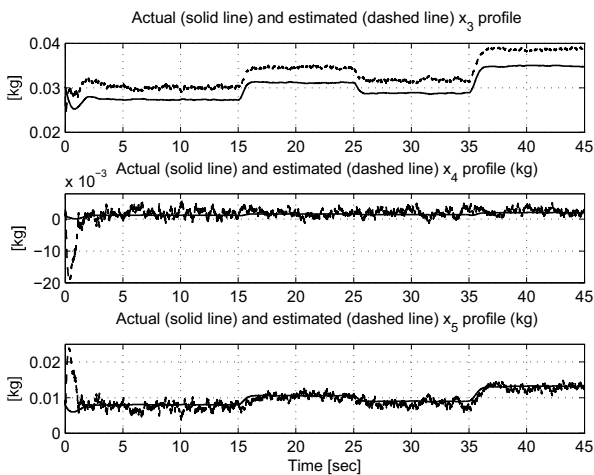
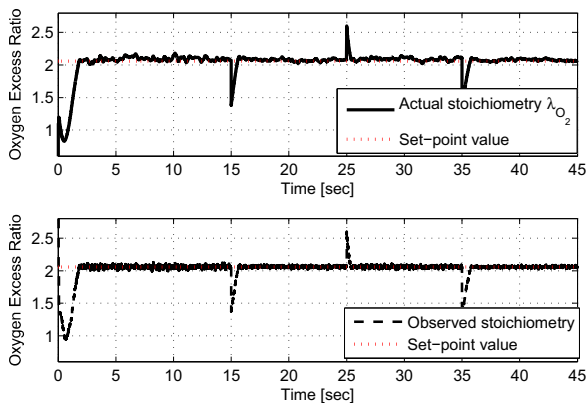

 Fig. 6. Actual and observed profiles of variables x_3, x_4, x_5 in TEST 3

 Fig. 7. Actual and observed λ_{O_2} , and set-point value, in TEST 3


Fig. 8. Stoichiometry steady-state behavior in TEST 3

lowing [5], uncertainties up to the 10% of the nominal value were taken into account, as listed in Table II. Figure 6 shows the actual and estimated profiles of the unmeasured variables x_3, x_4, x_5 . The main deterioration in the observer performance reveals in a biased observation of the x_3 variable (the air mass in the supply manifold) while the estimates of the remaining unmeasured variables x_4, x_5 keep relatively accurate in the face of the parameter errors. Figure 7 shows that the performance of the observer based stoichiometry controller remains satisfactory. The sliding variable time history and zoom, shown in the Figures 8, show minor changes as compared to the previous TEST 2, confirming the robustness of the adopted design.


 Fig. 9. Noisy and noise-free measurements of x_1 , x_2 , x_6 and I_{st} in TEST 4

 Fig. 10. Actual and observed profiles of variables x_3 , x_4 , x_5 in TEST 4

 Fig. 11. Actual and observed λ_{O_2} , and set-point value, in TEST 4

In particular, the magnitude of the stoichiometry oscillation (see Figure 8-bottom) remains close to the required value of 2×10^{-3} .

In the conclusive TEST 4, a realistic measurement noise has been included in addition to the parameter uncertainty. Considering that common values of signal-to-noise ratio (SNR) in data-acquisition systems are about 90 [dB] [44], all measurements, were converted into the $(4 \div 20\text{mA})$ range with power transmission equal to $P = 0.2$ [W], and then an additive gaussian noise with $\text{SNR} = 80$ [dB] was included. Figure (9) reports the noisy and noise-free profiles of all the measured quantities, showing that a remarkable level of noise was in fact taken into account. Figure (10) shows the actual and observed profiles of the unmeasured quantities, showing that the only visible effect of the noise, as compared to TEST 3, is the appearance of small oscillations of the observed x_4 and x_5 profiles. Figure (11) shows the actual and estimated stoichiometry, confirming that the proposed scheme works accurately also in the simultaneous presence of noise and parameter uncertainties.

VI. CONCLUSIONS

In this paper an observer-based controller has been proposed for regulating the oxygen excess ratio of a PEM FC to a suitable constant set-point value. The nonlinear observer, whose design constitutes one of the original contributions of the present paper, contains an output injection term based on an original combination between second- and third-order SM control algorithms, and it provides a finite-time converging and theoretically exact (in absence of noise and parameter errors) state reconstruction. The control loop, which uses the observed oxygen excess ratio, is also based on the SOSM approach. To tune the controller parameters it has been adopted a novel procedure, supported by local linearization and frequency domain arguments, which allows the designer to affect the steady state behavior of the output response in a quite direct and transparent manner. The overall approach has been successfully demonstrated by thorough simulative analysis considering relevant practical implementation issues such as parameter uncertainty and measurement noise. Next activities will be targeted to carry out experimental tests, on one hand, and to consider as well more complex mathematical models of the PEM FC, such as distributed parameter ones, which can capture more accurately the complex transport and reaction phenomena taking place inside the FC.

VII. APPENDIX

A. State-Space PEM FC Model Equations

$$\begin{aligned}
 \dot{x}_1 &= (\tau_{cm}(u, x_1) - \tau_{cp}(x_1, x_2)) / J_{cp} \\
 \dot{x}_2 &= (\gamma R_a / V_{sm}) \times (T_{cp}(x_2) W_{cp}(x_1, x_2) - T_{sm}(x_2, x_3) \times \\
 &\quad W_{sm, out}(x_2, x_4, x_5)) \\
 \dot{x}_3 &= W_{cp}(x_1, x_2) - W_{sm, out}(x_2, x_4, x_5) \\
 \dot{x}_4 &= W_{O_2, in}(x_2, x_4, x_5) - W_{O_2, out}(x_4, x_5, x_6) - W_{O_2, react}(I_{st}) \\
 \dot{x}_5 &= W_{N_2, in}(x_2, x_4, x_5) - W_{N_2, out}(x_4, x_5, x_6) \\
 \dot{x}_6 &= R_a T_{fc} (W_{ca, out}(x_4, x_5, x_6) - W_{rm, out}(x_6)) / (V_{rm} M_a)
 \end{aligned}$$

B. Physical functions

- Accelerating and Load Torque

$$\begin{aligned}
 \tau_{cm}(u, x_1) &= n_{cm} K_t (u - K_v x_1) / (R_{cm} J_{cp}) \\
 \tau_{cp}(x_1, x_2) &= C_p T_{atm} n(x_2) W_{cp}(x_1, x_2) / (n_{cp} J_{cp} x_1)
 \end{aligned}$$

- Supply Manifold and Compressor Air temperatures

$$\begin{aligned} T_{cp}(x_2) &= T_{atm}(1+n(x_2)n_{cp}^{-1}) \\ T_{sm}(x_2, x_3) &= V_{sm}x_2/(R_a x_3) \end{aligned}$$

- Mass flow rates

$$\begin{aligned} W_{cp}(x_1, x_2) &= C_{00} + C_{10}x_1 + C_{20}x_1^2 + C_{01}x_2 \\ &\quad + C_{11}x_1x_2 + C_{02}x_2^2 \\ W_{sm,out}(x_2, x_4, x_5) &= K_{sm,out}(x_2 - p_{v,ca} - R_{N_2}T_{st}x_5/V_{ca} \\ &\quad - R_{O_2}T_{st}x_4/V_{ca}) \\ W_{O_2,in}(x_2, x_3, x_4) &= ((x_2 - B_{32} - B_{33} - x_5B_{34} - x_4B_{35}) \times \\ &\quad (x_2 - x_2B_6)^{-1} + (x_2B_{36} - B_{37} - x_5B_{38} \\ &\quad - x_4B_{39}))e(x_2)k(x_2) \\ W_{O_2,out}(x_4, x_5, x_6) &= -x_4(B_{10} - x_5B_{11} + x_4B_{12} - x_6B_9) \times \\ &\quad j(x_4, x_5)x_4^{-1}(j(x_4, x_5)B_{40} - M_{N_2})^{-1} \times \\ &\quad m(x_4, x_5) \\ W_{N_2,in}(x_2, x_3, x_4) &= ((x_2B_{23} - B_{24} - x_5B_{25} - x_4B_{26}) \times \\ &\quad (x_2 - x_2B_6)^{-1} + (x_2B_{27} - B_{28} - x_5B_{29} \\ &\quad - x_4B_{30}))e(x_2)k(x_2) \\ W_{N_2,out}(x_4, x_5, x_6) &= (1 - j(x_4, x_5)B_{15}(j(x_4, x_5)B_{41} + M_{N_2})^{-1}) \\ &\quad \times (B_{20} + x_5B_{21} + x_4B_{22} - x_6B_{19})m(x_4, x_5) \\ W_{ca,out}(x_4, x_5, x_6) &= B_{47} + x_5B_{48} + x_4B_{49} - x_6B_{46} \\ W_{rm,out}(x_6) &= p_{a6} + p_{a5}c(x_6) + p_{a4}c(x_6)^2 + p_{a3}c(x_6)^3 \\ &\quad + p_{a2}c(x_6)^4 + p_{a1}c(x_6)^5 \end{aligned}$$

C. Auxiliary functions

$$\begin{aligned} e(x_2) &= \left(1 + \frac{x_2B_5}{x_2 - x_2B_6}\right)^{-1}; \quad c(x_6) = \frac{x_6 - \text{mean}_a}{\text{std}_a}; \\ j(x_4, x_5) &= \frac{x_4}{x_5B_{13} + x_4B_{14}}; \quad n(x_2) = \left(\frac{x_2}{p_{atm}}\right)^{(\gamma-1)/\gamma} - 1; \\ k(x_2) &= \left(1 + \frac{B_7}{x_2 - x_2B_6 + B_8}\right)^{-1}; \\ m(x_4, x_5) &= (1 + B_{31}(j(x_4, x_5)B_{41} + M_{N_2})^{-1}j(x_4, x_5)x_4^{-1})^{-1} \end{aligned}$$

D. Polynomial Coefficients of W_{cp} and $W_{rm,out}$ [32]

$C_{00} = 4.83 \times 10^{-5}$; $C_{10} = -5.42 \times 10^{-5}$; $C_{20} = 8.79 \times 10^{-6}$; $C_{01} = 3.49 \times 10^{-7}$; $C_{11} = 3.55 \times 10^{-13}$; $C_{02} = -4.11 \times 10^{-10}$; $p_{a1} = 0.0012$; $p_{a2} = -0.0019$; $p_{a3} = -0.0015$; $p_{a4} = 0.0021$; $p_{a5} = 0.027$; $p_{a6} = 0.078$.

E. Ford 75-kW P2000 FC stack Physical Parameters [4]

$\gamma = 1.4$; $\theta = T_{cp,in}/T_{amb}$; $\phi_{atm} = 0.5$; $\phi_{ca,in} = 1$; $\phi_{des} = 1$; $\phi_{max} = 1.55 \times 10^{-3}$; $\Phi_{max} = 0.197$; $d_c = 0.2286$; $ef_{mec} = 0.9$; $K_{ca,out} = 2.17 \times 10^{-6}$; $m_{v,ca,max} = 0.0028$; $\text{mean}_a = 2.5 \times 10^5$; $n = 381$; $n_{cm} = 1$; $n_{cp} = 0.775$; $p_{amb} = 1$; $p_{atm} = 101325$; $p_{cp,in} = p_{amb}$; $p_{sat,T_{atm}} = 3.14 \times 10^3$; $p_{sat,T_{cl}} = 47.06 \times 10^3$; $p_{v,ca} = m_{v,ca,max}R_vT_{st}/V_{ca}$; $\text{std}_a = 8.66 \times 10^4$; $C_p = 1004$; $F = 96485$; $J_{cp} = 5 \times 10^{-5}$; $K_{sm,out} = 0.36 \times 10^{-5}$; $K_v = 0.0153$; $M_a = 28.84 \times 10^{-3}$; $M_{N_2} = 28 \times 10^{-3}$; $M_{O_2} = 32 \times 10^{-3}$; $M_v = 18.02 \times 10^{-3}$; $R_a = 2.869 \times 10^2$; $R_{cm} = 1.2$; $R_{O_2} = 259.8$; $R_{N_2} = 296.8$; $R_v = 461.5$; $T_{amb} = 298$; $T_{atm} = T_{amb}$; $T_{cp,in} = T_{amb}$; $T_{st} = 353$; $T_{fc} = T_{st}$; $V_{ca} = 0.01$; $V_{rm} = 0.005$; $V_{sm} = 0.02$; $X_{O_2,ca,in} = (Y_{O_2,ca,in}M_{O_2})/(Y_{O_2,ca,in}M_{O_2} + (1 - Y_{O_2,ca,in})M_{N_2})$; $Y_{O_2,ca,in} = 0.21$.

F. Auxiliary Coefficients

$B_1 = M_v\phi_{des}p_{sat,T_{cl}}K_{sm,out}/M_a$; $B_2 = B_1p_{v,ca}$; $B_3 = B_1R_{N_2}T_{st}/V_{ca}$; $B_4 = B_1R_{O_2}T_{st}/V_{ca}$; $B_5 = M_v\phi_{atm}p_{sat,T_{atm}}/(M_a p_{atm})$; $B_6 = \phi_{atm}p_{sat,T_{atm}}/p_{atm}$; $B_7 = M_v\phi_{ca,in}p_{sat,T_{cl}}(Y_{O_2,ca,in}M_{O_2} + (1 - Y_{O_2,ca,in})M_{N_2})^{-1}$; $B_8 = \phi_{des}p_{sat,T_{cl}} - \phi_{ca,in}p_{sat,T_{cl}}$; $B_9 = R_{O_2}T_{st}M_{O_2}K_{ca,out}/V_{ca}$; $B_{10} = B_9p_{v,ca}$; $B_{11} = B_9R_{N_2}T_{st}/V_{ca}$; $B_{12} = B_9R_{O_2}T_{st}/V_{ca}$; $B_{13} = R_{N_2}T_{st}/V_{ca}$; $B_{14} = R_{O_2}T_{st}/V_{ca}$; $B_{15} = B_9/K_{ca,out}$; $B_{16} = R_{O_2}T_{st}M_{N_2}/V_{ca}$; $B_{17} = M_{O_2}n/(F4)$; $B_{18} = 1 - Y_{O_2,ca,in}M_{O_2}/(Y_{O_2,ca,in}M_{O_2} + (1 - Y_{O_2,ca,in})M_{N_2})$; $B_{19} = K_{ca,out}$; $B_{20} = K_{ca,out}p_{v,ca}$; $B_{21} = K_{ca,out}R_{N_2}T_{st}/V_{ca}$; $B_{22} = K_{ca,out}R_{O_2}T_{st}/V_{ca}$; $B_{23} = B_{18}B_1$; $B_{24} = B_{23}p_{v,ca}$; $B_{25} = B_{23}B_{13}$; $B_{26} = B_{23}B_{14}$; $B_{27} = B_{18}K_{sm,out}$

$B_{28} = B_{18}p_{v,ca}$; $B_{29} = B_{18}R_{N_2}T_{st}/V_{ca}$; $B_{30} = B_{18}R_{O_2}T_{st}/V_{ca}$; $B_{31} = M_vp_{v,ca}$; $B_{32} = X_{O_2,ca,in}B_1$; $B_{33} = X_{O_2,ca,in}B_2$; $B_{34} = X_{O_2,ca,in}B_3$; $B_{35} = X_{O_2,ca,in}B_4$; $B_{36} = X_{O_2,ca,in}K_{sm,out}$; $B_{37} = X_{O_2,ca,in}p_{v,ca}$; $B_{38} = X_{O_2,ca,in}R_{N_2}T_{st}/V_{ca}$; $B_{39} = X_{O_2,ca,in}R_{O_2}T_{st}/V_{ca}$; $B_{40} = B_{15} - B_{16}$; $B_{41} = B_{14}M_{O_2} - B_{16}$; $B_{42} = 14 \times 2C_pT_{cp,in}(d_c/(2\sqrt{\theta}))^{-2}\Phi_{max}^{-1}$.

REFERENCES

- [1] R. J. Talj, D. Hissel, R. Ortega, M. Becherif, and M. Hilairet, "Experimental validation of a pem fuel-cell reduced-order model and a moto-compressor higher order sliding-mode control," *IEEE Trans. Ind. Electron.*, vol. 57, no. 6, pp. 1906–1913, 2010.
- [2] F. Barbir and S. Yazici, "Status and development of pem fuel cell technology," *International Journal of Energy Research*, vol. 32, no. 5, pp. 369–378, 2008.
- [3] C. A. Ramos-Paja, R. Giral, L. Martinez-Salamero, J. Romano, A. Romero, and G. Spagnuolo, "A pem fuel-cell model featuring oxygen-excess-ratio estimation and power-electronics interaction," *IEEE Trans. Ind. Electron.*, vol. 57, no. 6, 2010.
- [4] C. Kunusch, P. F. Puleston, M. A. Mayosky, and A. Dávila, "Efficiency optimisation of an experimental pem fuel cell system via super twisting control," in *Variable Structure Systems (VSS), 2010 11th International Workshop on*. IEEE, 2010, pp. 319–324.
- [5] C. Kunusch, P. F. Puleston, M. A. Mayosky, and J. Riera, "Sliding mode strategy for pem fuel cells stacks breathing control using a super-twisting algorithm," *IEEE Trans. Control Syst. Technol.*, vol. 17, no. 1, pp. 167–174, 2009.
- [6] C. Kunusch, P. Puleston, and M. Mayosky, *Sliding-Mode Control of PEM Fuel Cells*. Springer, 2012.
- [7] C. Kunusch, P. F. Puleston, M. A. Mayosky, and L. Fridman, "Experimental results applying second order sliding mode control to a pem fuel cell based system," *Control Eng. Practice*, vol. 21, no. 5, 2013.
- [8] A. Arce, A. J. del Real, C. Bordons, and D. R. Ramirez, "Real-time implementation of a constrained mpc for efficient airflow control in a pem fuel cell," *IEEE Trans. Ind. Electron.*, vol. 57, no. 6, pp. 1892–1905, 2010.
- [9] M. Grujicic, K. Chittajallu, and J. Pukrushpan, "Control of the transient behaviour of polymer electrolyte membrane fuel cell systems," *Proc. of the Institution of Mechanical Engineers, Part D: Journal of Automobile Eng.*, vol. 218, no. 11, pp. 1239–1250, 2004.
- [10] M. Schultze and J. Horn, "State estimation for pem fuel cell systems with time delay by an unscented kalman filter and predictor strategy," in *Control & Automation (MED), 2013 21st Mediterranean Conf. on*. IEEE, 2013, pp. 104–112.
- [11] E.-S. Kim, C.-J. Kim, and K.-S. Eom, "Nonlinear observer design for pem fuel cell systems," in *Electrical Machines and Systems, 2007. ICEMS. International Conf. on*. IEEE, 2007, pp. 1835–1839.
- [12] P. Vijay, M. O. Tade, K. Ahmed, R. Utikar, and V. Pareek, "Simultaneous estimation of states and inputs in a planar solid oxide fuel cell using nonlinear adaptive observer design," *Journal of Power Sources*, vol. 248, pp. 1218–1233, 2014.
- [13] I. H. Kazmi and A. I. Bhatti, "Parameter estimation of proton exchange membrane fuel cell system using sliding mode observer," *International Journal of Innovative Computing, Information and Control*, vol. 8, no. 7B, pp. 5137–5148, 2012.
- [14] I. Kazmi, A. Bhatti, and M. Iqbal, "Parameter estimation of pemfc system with unknown input," in *Variable Structure Systems (VSS), 2010 11th International Workshop on*. IEEE, 2010, pp. 301–306.
- [15] E.-S. Kim, C.-J. Kim, and K.-S. Eom, "Nonlinear observer design for pem fuel cell systems," in *Electrical Machines and Systems, 2007. ICEMS. International Conf. on*. IEEE, 2007, pp. 1835–1839.
- [16] Y. B. Shtessel, S. Baev, C. Edwards, and S. Spurgeon, "Hosm observer for a class of non-minimum phase causal nonlinear mimo systems," *IEEE Trans. Autom. Control*, vol. 55, no. 2, pp. 543–548, 2010.
- [17] B. Cannas, S. Cincotti, and E. Usai, "A chaotic modulation scheme based on algebraic observability and sliding mode differentiators," *Chaos, Solitons & Fractals*, vol. 26, no. 2, pp. 363–377, 2005.
- [18] J. Davila, L. Fridman, A. Pisano, and E. Usai, "Finite-time state observation for non-linear uncertain systems via higher-order sliding modes," *Int. Journal of Control*, vol. 82, no. 8, pp. 1564–1574, 2009.
- [19] J. Davila, H. Rios, and L. Fridman, "State observation for nonlinear switched systems using nonhomogeneous high-order sliding mode observers," *Asian Journal of Control*, vol. 14, no. 4, pp. 911–923, 2012.

- [20] L. Fridman, A. Levant, and J. Davila, "Observation of linear systems with unknown inputs via high-order sliding-modes," *International Journal of Systems Science*, vol. 38, no. 10, pp. 773–791, 2007.
- [21] A. Pilloni, E. Usai, C. Edwards, A. Pisano, and P. P. Menon, "Decentralized state estimation in connected systems," in *5th Symposium on System Structure and Control*. IFAC, 2013, pp. 421–426.
- [22] S. M. Rakhtala, A. R. Noei, R. Ghaderi, and E. Usai, "Design of finite-time high-order sliding mode state observer: A practical insight to pem fuel cell system," *Journal of Process Control*, vol. 24, no. 1, 2014.
- [23] J. Moreno, "Lyapunov function for levant's second order differentiator," in *Decision and Control (CDC), 2012 IEEE 51st Annual Conf. on*, 2012.
- [24] J. Moreno and D. Dochain, "Finite time converging input observers for nonlinear second-order systems," in *Decision and Control (CDC), 2013 IEEE 52nd Annual Conf. on*, 2013.
- [25] J. A. Moreno, "A lyapunov approach to output feedback control using second-order sliding modes," *IMA Journal of Mathematical Control and Information*, p. dnr036, 2012.
- [26] A. Levant, "Sliding order and sliding accuracy in sliding mode control," *International journal of control*, vol. 58, no. 6, pp. 1247–1263, 1993.
- [27] A. Pisano, D. Salimbeni, E. Usai, S. Rakhtala, and A. Noei, "Observer-based output feedback control of a pem fuel cell system by high-order sliding mode technique," in *Control Conf. (ECC), 2013 European*. IEEE, 2013, pp. 2495–2500.
- [28] I. Boiko, "Analysis of closed-loop performance and frequency-domain design of compensating filters for sliding mode control systems," *IEEE Trans. Autom. Control*, vol. 52, no. 10, pp. 1882–1891, 2007.
- [29] A. Pisano and E. Usai, "Contact force regulation in wire-actuated pantographs via variable structure control and frequency-domain techniques," *International Journal of Control*, vol. 81, no. 11, 2008.
- [30] A. Pilloni, A. Pisano, and E. Usai, "Oscillation shaping in uncertain linear plants with nonlinear pi control: Analysis and experimental results," in *Advances in PID Control*, vol. 2, no. 1, 2012, pp. 116–121.
- [31] J. T. Pukrushpan, A. G. Stefanopoulou, and H. Peng, "Control of fuel cell breathing," *IEEE Control Syst. Mag.*, vol. 24, no. 2, pp. 30–46, 2004.
- [32] C. Kunusch, P. F. Puleston, M. A. Mayosky, and A. P. Husar, "Control-oriented modeling and experimental validation of a pemfc generation system," *IEEE Trans. Energy Convers.*, vol. 26, no. 3, 2011.
- [33] J. T. Pukrushpan, A. G. Stefanopoulou, and H. Peng, *Control of fuel cell power systems: principles, modeling, analysis and feedback design*. Springer, 2004.
- [34] A. Niknezhadi, M. Allué-Fantova, C. Kunusch, and C. Ocampo-Martínez, "Design and implementation of lqr/lqg strategies for oxygen stoichiometry control in pem fuel cells based systems," *Journal of Power Sources*, vol. 196, no. 9, pp. 4277–4282, 2011.
- [35] "Product catalog of the multi parameter gas mass flow meter." Omega Engineering®, 2013. [Online]. Available: <http://www.omega.com>
- [36] I. Boiko, *Discontinuous Control Systems: Frequency-Domain Analysis and Design*. Springer, 2008.
- [37] A. Levant and L. M. Fridman, "Accuracy of homogeneous sliding modes in the presence of fast actuators," *IEEE Trans. Autom. Control*, vol. 55, no. 3, p. 810, 2010.
- [38] I. Boiko, L. Fridman, and R. Iriarte, "Analysis of chattering in continuous sliding mode control," in *American Control Conf., 2005. Proc. of the 2005*. IEEE, 2005, pp. 2439–2444.
- [39] O. A. Ameri and I. Boiko, "Analysis of performance of a liquid level process controlled by the super-twisting algorithm," in *Control Conf. (ECC), 2013 European*. IEEE, 2013, pp. 3222–3227.
- [40] B. Belvedere, M. Bianchi, A. Borghetti, A. De Pascale, M. Di Silvestro, and M. Paolone, "Dsp-controlled test set-up for the performance assessment of an autonomous power unit equipped with a pem fuel cell," in *Clean Electr. Power, ICCEP'07. Int. Conf. on*. IEEE, 2007.
- [41] "Compactrio reference and procedures help (fpga interface)." 2010. [Online]. Available: www.ni.com/dataacquisition/compactrio/
- [42] "Pci-1710u series user manual," 2013. [Online]. Available: www.messcomp.com/manual/40691302.pdf
- [43] C. Bao, K. Zhang, M. Ouyang, B. Yi, and P. Ming, "Dynamic test and real-time control platform of anode recirculation for pem fuel cell systems," *J. of fuel cell science and tech.*, vol. 3.3, pp. 333–345, 2006.
- [44] M. Pachchigar, "Complete sensor-to-bits solution simplifies industrial data-acquisition system design," *Analog Dialogue: Technical magazine of Analog Devices.*, vol. 47, no. 2, pp. 21–24, 2013.



Alessandro Pilloni was born in 1984. He received Laurea degree (with honors) in electronic engineering and the Ph.D. degree in industrial engineering from the University of Cagliari (Italy), respectively in 2010 and 2014. He currently holds a research fellow position at the Department of Electrical and Electronic Engineering of the same university. His research area includes variable structure control theory and their applications to nonlinear, uncertain and/or distributed parameter systems, fault-detection, output regulation, consensus and synchronization of coupled dynamical systems. He has spent visiting periods at Universities and Research Centers in Spain, United Kingdom and Serbia. Dr. Pilloni is a member of SICC (Italian Society of Chaos and Complexity). He is reviewer for several international conferences and journals, such as IEEE Transaction on Automatic Control, IEEE Transactions on Control Systems Technology, Automatica (Elsevier) and many other.



Alessandro Pisano was born in 1972. He graduated in Electronic Engineering in 1997 at the Department of Electrical and Electronic Engineering (DIEE) of the Cagliari University (Italy), where he received the Ph.D. degree in Electronics and Computer Science in 2000. He currently holds a position as assistant professor at DIEE. His current research interests include nonlinear control theory and its applications to nonlinear, uncertain and/or distributed parameter systems. He has authored/co-authored one book, 57 journal publications, 10 book chapters, and 105 papers in peer-reviewed international conference proceedings, and he is the holder of 4 patents. He has spent visiting periods at Universities and Research Centers in Belgium, France, Serbia and Mexico. Dr. Pisano is a member of IEEE and a Professional Engineer registered in Cagliari, Italy. He is Associate Editor of the Asian Journal of Control and of the IEEE Control Systems Society Conference Editorial Board.



Elio Usai is currently associate professor at the Department of Electrical and Electronic Engineering (DIEE)-University of Cagliari, where he received the Laurea degree (MSc) in Electrical Engineering in 1985. He worked as process engineer first and then as production manager for international companies until September 1994, when he joined DIEE as an assistant professor. His first research interest was on parameter identification in nonlinear systems and on optimal control. Current interests are in output-feedback control, state estimation and FDI via higher order sliding modes in linear, nonlinear and infinite dimensional systems. He is co-author of more than 150 articles in international journals and conferences. He was General Chairperson of VSS'06, and he currently is Associate Editor for Asian J. of Control and IEEE Trans. on Control System Technology. He is/was the leader of research projects on the control of uncertain systems and on model based fault detection.